Physics

Physics Research Publications

Purdue University *Year* 2006

Multiwavelength observations of 1ES 1959+650, 1 year after the strong outburst of 2002

K. Gutierrez, H. M. Badran, S. M. Bradbury, J. H. Buckley, O. Celik, Y. C. Chow, P. Cogan, W. Cui, M. Daniel, A. Falcone, S. J. Fegan, J. P. Finley, G. H. Gillanders, J. Grube, J. Holder, D. Horan, S. B. Hughes, I. Jung, D. Kieda, K. Kosack, H. Krawczynski, F. Krennrich, M. J. Lang, S. Le Bohec, G. Maier, P. Moriarty, J. Perkins, M. Pohl, J. Quinn, P. F. Rebillot, H. J. Rose, M. Schroedter, G. H. Sembroski, S. P. Wakely, T. C. Weekes, and R. J. White

The Astrophysical Journal, 644:742–747, 2006 June 20

MULTIWAVELENGTH OBSERVATIONS OF 1ES 1959+650, 1 YEAR AFTER THE STRONG OUTBURST OF 2002

K. Gutierrez,[1] H. M. Badran,[2] S. M. Bradbury,[3] J. H. Buckley,[1] O. Celik,[4] Y. C. Chow,[4] P. Cogan,[5] W. Cui,[6] M. Daniel,[5] A. Falcone,[6] S. J. Fegan,[4] J. P. Finley,[6] G. H. Gillanders,[5] J. Grube,[3] J. Holder,[3] D. Horan,[7] S. B. Hughes,[1] I. Jung,[1] D. Kieda,[8] K. Kosack,[1] H. Krawczynski,[1] F. Krennrich,[9] M. J. Lang,[5] S. Le Bohec,[8] G. Maier,[3] P. Moriarty,[10] J. Perkins,[1] M. Pohl,[9] J. Quinn,[5] P. F. Rebillot,[1] H. J. Rose,[3] M. Schroedter,[4,7] G. H. Sembroski,[6] S. P. Wakely,[11] T. C. Weekes,[7] and R. J. White[3] (The VERITAS Collaboration)

and

M. Aller,[12] H. Aller,[12] P. Charlot,[13] and J. F. Le Campion[13]

Received 2005 September 26; accepted 2006 February 27

ABSTRACT

In 2003 April–May, the blazar 1ES 1959+650 showed an increased level of X-ray activity. This prompted a multiwavelength observation campaign with the Whipple 10 m γ-ray telescope, the *Rossi X-Ray Timing Explorer*, the Bordeaux Optical Observatory, and the University of Michigan Radio Astronomy Observatory. We present the multiwavelength data taken from 2003 May 2 to June 7 and compare the source characteristics with those measured during observations taken during the years 2000 and 2002. The X-ray observations gave a data set with high signal-to-noise ratio light curves and energy spectra; however, the γ-ray observations did not reveal a major TeV γ-ray flare. Furthermore, we find that the radio and optical fluxes do not show statistically significant deviations from those measured during the 2002 flaring periods. While the X-ray flux and X-ray photon index appear correlated during subsequent observations, the apparent correlation evolved significantly among the years 2000, 2002, and 2003. We discuss the implications of this finding for the mechanism that causes the flaring activity.

Subject headings: BL Lacertae objects: individual (1ES 1959+650) — galaxies: jets — gamma rays: observations

1. INTRODUCTION

Blazars are a class of active galactic nuclei (AGNs) with collimated plasma outflows (jets) directed along the line of sight. The jets give rise to a continuum emission extending from the radio to X-rays, sometimes even into the MeV and GeV/TeV energy range. The blazar 1ES 1959+650 is 1 of 10 blazars detected so far in the GeV/TeV energy range with ground-based Cerenkov telescopes (Krawczynski 2006; Tavecchio 2006). With a redshift $z = 0.047$ (Schachter et al. 1993), it is farther away from us than the two strongest TeV γ-ray sources, Mrk 421 ($z = 0.031$) and Mrk 501 ($z = 0.034$), but substantially closer than the recently detected TeV emitters H 2356−309 ($z = 0.165$) and 1ES 1101−232 ($z = 0.186$).

In the year 2002, 1ES 1959+650 went into a state of high TeV γ-ray activity (Holder et al. 2003; Aharonian et al. 2003) and was observed intensively with good multiwavelength coverage (Krawczynski et al. 2004, hereafter Paper I). The source showed very hard X-ray energy spectra with 3–25 keV photon indices Γ ($dN/dE \propto E^{-\Gamma}$) between 1.6 and 2.4 (Paper I). The fact that its spectral energy distribution (SED) peaks sometimes at energies well above 15 keV makes the source one of the most extreme synchrotron blazars, similar to Mrk 501 (Pian et al. 1998) and 1H 1426+428 (Falcone et al. 2004).

The time-averaged TeV γ-ray energy spectrum from the flaring period of 2002 has been fitted with a power-law model, giving a photon index Γ of 2.8 over the energy range from 316 GeV to 10 TeV (Aharonian et al. 2003; Daniel et al. 2005). Although the TeV γ-ray spectrum of 1ES 1959+650 is steeper than that of Mrk 501 in its high state ($\Gamma \approx 2.2$; Aharonian et al. 1999), the difference may be entirely caused by the larger redshift of the source and hence the larger extent of extragalactic absorption in pair production processes of the TeV γ-rays with photons from the cosmic infrared background (CIB; Schroedter 2005).

It is interesting to note that the source showed an "orphan" flare (a flare in the TeV γ-ray band without a corresponding flare in the X-ray band) on 2002 June 4. While the TeV flux increased from 0.26 ± 0.21 times the flux of the Crab Nebula to about 4 times the flux of the Crab Nebula within 5 hours, the X-ray flux, X-ray photon index, and optical brightness stayed approximately constant. This 2002 observation challenges simple one-zone synchrotron self-Compton (SSC) models in which the

[1] Department of Physics, Washington University, St. Louis, MO 63130.
[2] Physics Department, Tanta University, Tanta, Egypt.
[3] School of Physics and Astronomy, University of Leeds, Leeds LS2 9JT, Yorkshire, England, UK.
[4] Department of Physics, University of California, Los Angeles, CA 90095-1562.
[5] Department of Physics, National University of Ireland, Galway, Ireland.
[6] Department of Physics, Purdue University, West Lafayette, IN 47907.
[7] Fred Lawrence Whipple Observatory, Harvard-Smithsonian Center for Astrophysics, P.O. Box 97, Amado, AZ 85645-0097.
[8] High Energy Astrophysics Institute, University of Utah, Salt Lake City, UT 84112.
[9] Department of Physics and Astronomy, Iowa State University, Ames, IA 50011-3160.
[10] School of Science, Galway-Mayo Institute of Technology, Galway, Ireland.
[11] Enrico Fermi Institute, University of Chicago, Chicago, IL 60637.
[12] University of Michigan, Ann Arbor, MI 48109.
[13] Observatoire de Bordeaux (OASU)—CNRS/UMR 5804, BP 89, 33270 Floirac, France.

X-rays originate as synchrotron emission of a single relativistic electron population and the TeV γ-rays are produced from inverse Compton scattering of the synchrotron photons by the same population of electrons. Paper I discusses several possible explanations for the orphan flare: multiple emission zones contributing to the observed radiation, time-variable external seed photon fields for inverse Compton processes, an ordered magnetic field aligned with the jet axis, and hadronic rather than leptonic emission models. In a more recent paper, Böttcher (2005) studied the possibility that the orphan flare originated from relativistic protons ($\gamma_P = 10^3$–10^4) in $p\gamma \rightarrow \Delta^+ \rightarrow p\pi_0$ and $\pi_0 \rightarrow \gamma\gamma$ processes inside the jet as the protons interacted with jet photons backscattered into the jet by a cloud several parsecs from the central engine. He found that reasonable variations in the values of the model parameters explain all the data satisfactorily. A recent twist in the story of the orphan flare is its possible association with a $\sim$TeV neutrino detected by the AMANDA neutrino telescope from the direction of 1ES 1959+650 in temporal coincidence; however, the statistical significance cannot be reliably estimated (Halzen & Hooper 2005). If 1ES 1959+650 indeed emitted high-energy neutrinos, purely leptonic synchrotron-Compton models would be ruled out.

In this paper we report on multiwavelength observations of 1ES 1959+650 performed between 2003 May 2 and June 7. During the week preceding our observations, the all-sky monitor on board the *Rossi X-Ray Timing Explorer* (*RXTE*) satellite measured an elevated 2–12 keV flux on the order of 10 mcrab. We therefore invoked pointed *RXTE* observations and accompanying observations with the Whipple 10 m Cerenkov telescope, the Bordeaux optical telescope, and the University of Michigan Radio Astronomy Observatory (UMRAO). While the TeV γ-ray observations did not reveal any major TeV γ-ray flare and the radio and optical data did not show significant flux variability, we did acquire an X-ray data set with light curves and energy spectra with a high signal-to-noise ratio. We discuss the data sets in § 2 and present the multiwavelength light curves in § 3. We study the secular evolution, i.e., long-term evolution, of the X-ray/TeV γ-ray flux correlation and the X-ray flux versus X-ray spectral hardness correlation in § 4. We study the SED and fit it with a SSC model in § 5. We summarize and discuss the results in § 6, focusing on a very interesting result from the X-ray observations: a secular evolution of the possible X-ray flux versus an X-ray photon index correlation. Throughout the paper we compare results from 2003 with those obtained in 2002 (Paper I) and in earlier observations in 2000 (Giebels et al. 2002). In the following, fit results are given in the text and in the tables with 90% confidence interval errors; in figures, we show 1 σ error bars and 90% confidence level upper limits computed with the method described in Helene (1983).

2. DATA SETS AND DATA REDUCTION

Observations were taken with UMRAO between 2003 May 2 and June 29, with the Bordeaux optical telescope between 2003 June 7 and October 18, and with *RXTE* and the Whipple 10 m Cerenkov telescope between 2003 May 2 and June 7. Our X-ray observations added 34.5 ks of integration time to the 2000 data from Giebels et al. (2002) and the 2002 data from Paper I, which we reanalyze here. The TeV γ-ray data comprise 13.1 hr. Detailed descriptions of the data-cleaning and analysis procedures are given in Paper I and in Charlot & Le Campion (2004).

For the X-ray analysis, we use here the FTOOLS version 5.3.1 package for data cleaning and the Sherpa version 3.0.1 package for spectral fitting. Power-law and broken power-law models were fitted over the energy range from 4 to 15 keV, using a Galactic neutral hydrogen column density of 1.01×10^{21} cm^{-2}.[14] We exclude here the 3–4 keV data, as past experience has shown that it has a somewhat lower reliability than the 4–15 keV data. We limit the analysis of individual *RXTE* pointings to <15 keV (rather than to <25 keV as in Paper I), as the 15–25 keV band is dominated by Poissonian background fluctuations for the "low-flux" data sets from 2000 and 2003.

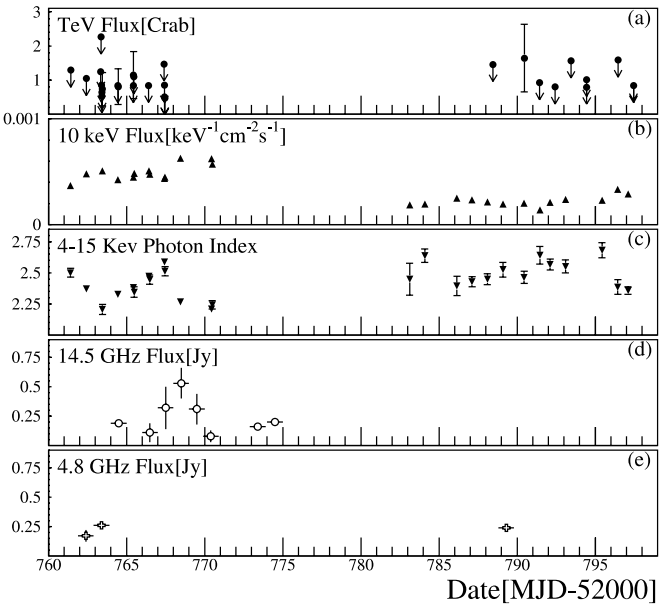

FIG. 1.—Results from the 1ES 1959+650 multiwavelength campaign (2003 May 2–June 7). (*a*) TeV γ-ray flux (Whipple) in crab units; the data are binned in 28 minute bins. (*b*) The 10 keV X-ray flux (*RXTE*). (*c*) The 4–15 keV X-ray photon index (*RXTE*). (*d*) The 14.5 GHz flux density (UMRAO). (*e*) The 4.8 GHz flux density (UMRAO).

We quote TeV fluxes as integral fluxes in units of the flux from the Crab Nebula. Given the zenith angle range of the observations, the peak energy of the flux measurements lies at 600 GeV.[15] Based on the Whipple measurements of the energy spectrum from the Crab Nebula (Hillas et al. 1998), a flux of 1 crab corresponds to a 1 TeV νF_ν flux of $(5.12 \pm 0.27_{\rm stat} \pm 0.96_{\rm syst}) \times 10^{-11}$ ergs cm^{-2} s^{-1}.

3. LIGHT CURVES

We briefly discuss here the light curves proceeding from short wavelengths to long wavelengths. The TeV γ-ray data (Fig. 1*a*) shows mostly upper limits. The observations did not reveal strong flares. Analyzing the entire TeV γ-ray data set, the significance of the γ-ray signal over the 2 month observation was 3.3 σ with a γ-ray rate of 0.24 ± 0.11 crab units. Thus, even on the longest accessible timescales, we have only marginal evidence for TeV γ-ray emission from the source. The large "gap" in the γ-ray light curve corresponds to the full Moon period when Cerenkov telescopes cannot be operated in standard mode and some additional down-time because of bad weather.

The 10 keV X-ray flux (Fig. 1*b*) varies by a factor of 3.4 over the course of the observations. The X-ray flux seems to

[14] This value was obtained at http://heasarc.gsfc.nasa.gov/cgi-bin/Tools/w3nh/w3nh.pl.

[15] The peak energy is defined as the energy at which the differential γ-ray detection rate peaks, assuming a source with the same spectrum as the Crab Nebula.

be correlated with the 4–15 keV photon index Γ (Fig. 1*c*) in the sense that higher fluxes are accompanied by harder energy spectra.

We do not show the optical data in Figure 1, as only one observation was taken during the multiwavelength campaign. During this one observation, the *V*-band optical magnitude was 15.27 ± 0.05 mag. The majority of optical observations were taken after the multiwavelength campaign. The flux measured during 54 nights between 2003 June 7 and October 18 varied between 14.89 and 15.67 mag, with an average of 15.21 ± 0.05 mag. During the 2002 flaring phase, the *V*-band magnitudes varied between 15.4 and 15.7 mag (Paper I). The combined 2002 and 2003 data thus show no evidence for correlation between the major X-ray/TeV γ-ray flaring phases and emission levels in the optical. The 14.5 and 4.8 GHz radio data are shown in Figures 1*d* and 1*e*, respectively. We do not show here the 8 GHz data, as they consist only of two data points. The radio data do not show significant evidence for flux variability, and the observed values are consistent with those measured earlier (Paper I; Gregory & Condon 1991; Becker et al. 1991). The data show that the fractional flux variability of 1ES 1959+650 in the radio band is 10% or less. Radio observations with higher sensitivity are needed to access any correlation between the radio fluxes and the X-ray or TeV γ-ray fluxes.

4. SECULAR EVOLUTION OF THE X-RAY/TeV FLUX CORRELATION AND THE X-RAY FLUX/SPECTRUM CORRELATION

The correlation between simultaneously measured TeV γ-ray and X-ray fluxes during the 2002 and 2003 observation campaigns is shown in Figure 2. The 2002 X-ray points are from our reanalysis of the data presented in Paper I. While the TeV γ-ray points are the same as in Paper I, we converted here all fluxes with a statistical significance below $1.6\,\sigma$ (90% confidence) into upper limits. One can recognize that the main difference between the 2002 and 2003 observations is a lack of strong X-ray and TeV γ-ray flares during the 2003 observations. Since both the X-ray and TeV γ-ray fluxes were lower in 2003 than in 2002, the data also do not show evidence for a correlation.

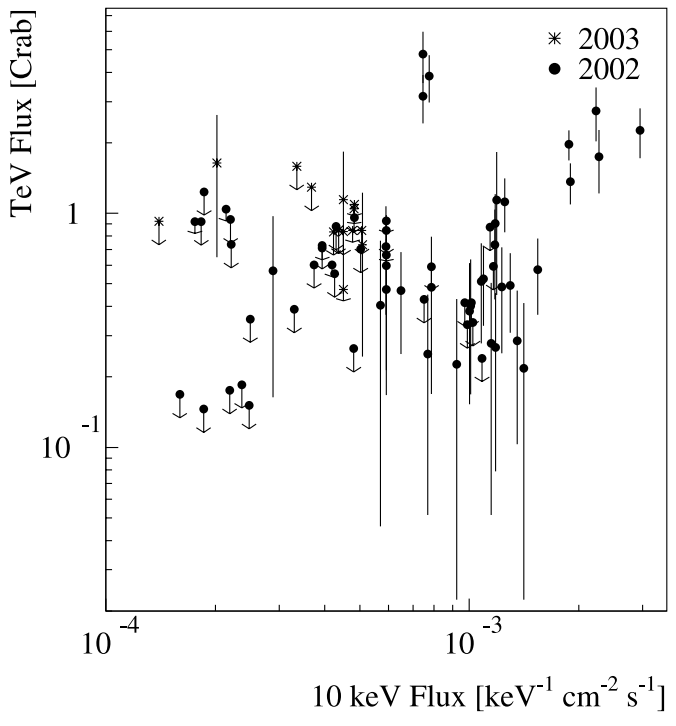

FIG. 2.—Correlation between the X-ray and TeV γ-ray fluxes for measurements within 2 hours of each other.

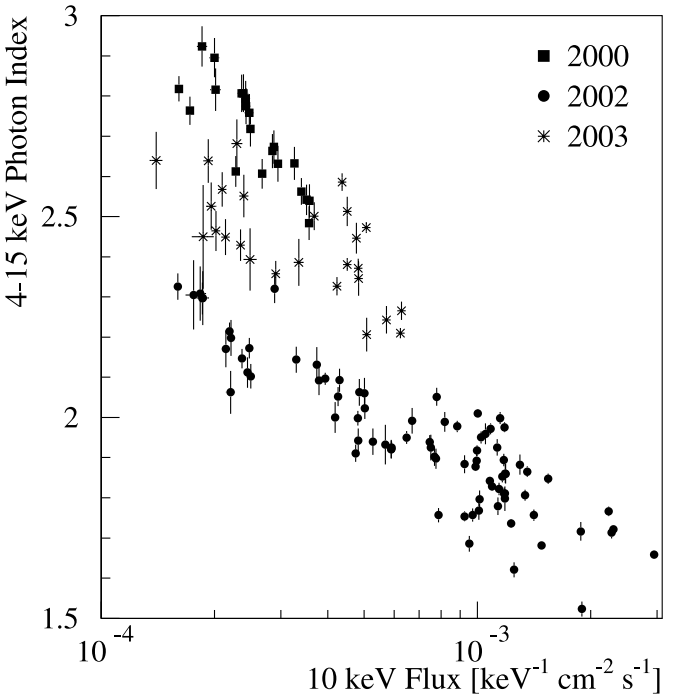

FIG. 3.—Correlation between the X-ray flux and the 4–15 keV photon index for observations in the years 2000, 2002, and 2003.

The X-ray flux versus X-ray photon index correlation is shown for the 2000, 2002, and 2003 data sets in Figure 3. The fluxes and photon indices appear to be correlated for the 2002 data set, and to a lesser extent in the 2003 data set; however, a secular evolution of the "correlation" can be recognized. For the same X-ray flux level, the energy spectrum was hardest during 2002, the year of the large X-ray and TeV γ-ray flares. We studied this effect further with a detailed spectral analysis in three flux bands. The June 2003 data, the entire 2000 data set, and a significant part of the 2002 data fit within a low 10 keV flux band of $(0.1-0.4)\times10^{-3}$ cm^{-2} s^{-1} keV^{-1}. A medium-flux band was chosen similarly and encompasses the 2003 May data and a portion of the 2002 data. Finally, a high-flux state represents the flaring data in 2002. Details of the combined spectra in these flux bands are given in Table 1. For the 2003 medium- and 2002 high-flux states the reduced χ^2 values are significantly better for either a cutoff power-law or log-parabolic model than a simple power law. Log-parabolic fits provide a direct way of calculating the peak in the total synchrotron spectrum. Figure 4 shows the 4–15 keV SEDs from Table 1 after applying a log-parabolic fit. The 2003 low- and medium-flux states give a peak synchrotron energy of 1.21 ± 0.64 and 1.09 ± 0.41 keV.

A similar short-term relationship between the photon index and the flux was found for Mrk 501 (Krawczynski et al. 2000). We discuss possible explanations for this type of secular evolution in § 6.

5. SED AND SSC MODELING

In Figure 5 we show the radio to γ-ray SED of 1ES 1959+650 together with results from simple one-zone SSC calculations.

TABLE 1
SPECTRAL FIT RESULTS FOR THE 4–15 keV DATA DIVIDED INTO THREE FLUX BANDS

Year	$F_{10\,\mathrm{keV}}$ (10^{-3} photons keV^{-1} cm^{-2} s^{-1})	χ^2_{Pow} [a]	χ^2_{Cut} [b]	χ^2_{Par} [c]	a [d]	b [e]	K [f]	E_p [g] (keV)	$\nu_p F(\nu_p)$ [h] (10^{-10} ergs cm^{-2} s^{-1})
2000.....	0.1–0.4	1.62	2.38	1.09	2.16 ± 0.12	0.28 ± 0.07	6.05 ± 0.63	0.51 ± 0.27	1.02 ± 0.13
2002.....	0.1–0.4	1.12	1.09	0.97	2.03 ± 0.08	0.11 ± 0.05	3.16 ± 0.23	0.71 ± 0.62	0.51 ± 0.04
	0.4–0.7	1.47	0.96	0.92	1.77 ± 0.06	0.13 ± 0.03	4.32 ± 0.24	6.76 ± 4.80	0.86 ± 0.12
	0.7–2.5	2.02	1.03	0.97	1.62 ± 0.04	0.14 ± 0.02	7.07 ± 0.31	20.4 ± 13.9	2.00 ± 0.36
2003.....	0.1–0.4	1.87	1.39	1.43	1.93 ± 0.17	0.38 ± 0.10	4.27 ± 0.63	1.21 ± 0.64	0.68 ± 0.10
	0.4–0.7	2.00	1.02	1.04	1.98 ± 0.07	0.23 ± 0.04	8.16 ± 0.57	1.09 ± 0.41	1.30 ± 0.09

[a] Reduced χ^2 value from 26 dof for a power-law fit.
[b] Reduced χ^2 value from 25 dof for a cutoff power-law fit.
[c] Reduced χ^2 value from 25 dof for a log-parabolic fit.
[d] Photon index for a log-parabolic fit.
[e] Curvature term for a log-parabolic fit.
[f] Flux normalization for a log-parabolic fit, in 10^{-2}.
[g] Peak energy from the log-parabolic fit.
[h] Peak flux from the log-parabolic fit.

The SSC code (Paper I) assumes a spherical emission volume of radius R moving with bulk Lorentz factor Γ_B toward the observer.[16] The emission volume is filled with an isotropic electron population and a randomly oriented magnetic field B. The energy spectrum of the electrons is assumed to be a broken power law from energy E_{min} to E_{max}, with differential spectral indices (p from $dn/dE \propto E^p$) of 2 and 3 below and above the break energy E_b. We use the CIB model of Kneiske et al. (2002) to calculate extragalactic absorption of the TeV γ-rays in pair production processes.

Figure 5 shows our SSC model with three different sets of parameter values: (1) the set of model parameter values from Paper I that describes an SED observed during 2002 at intermediate-flux levels, (2) the same model parameter values adapted to fit the 2003 SED by reducing the E_b and E_{max} values, and (3) an alternative fit to the 2003 data allowing free variation of the parameter values. Note that (1) and (2) produce almost identical inverse Compton components. The parameter values are summarized in Table 2. Explaining the differences between the 2002 and 2003 SEDs with a change of E_b and E_{max} alone results in

[16] The code can be downloaded on http://jelley.wustl.edu/multiwave/.

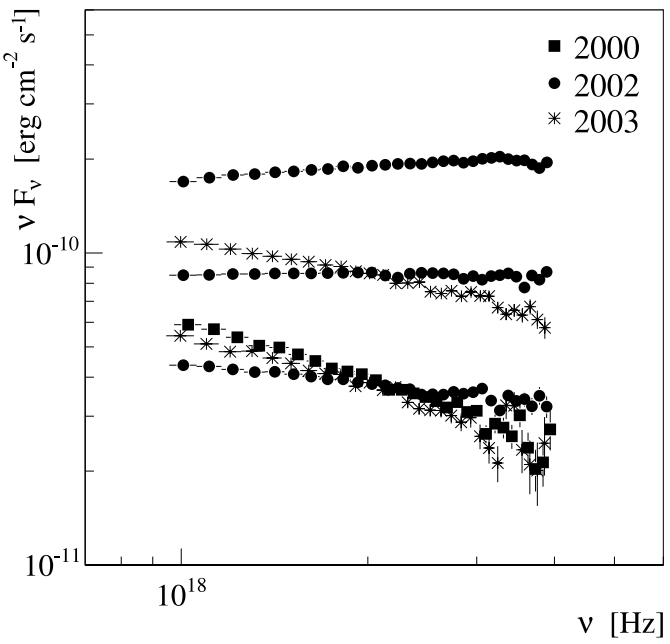

FIG. 4.—The 4–15 keV X-ray SEDs from combined spectra in three flux bands, from 2000, 2002, and 2003. The plot shows for each spectrum fitted the log-parabolic model multiplied by the number of counts detected in an energy bin divided by the number of counts expected in the bin, given the best-fit model parameters, and the statistical errors on the data scaled in this way. See Table 1 for details.

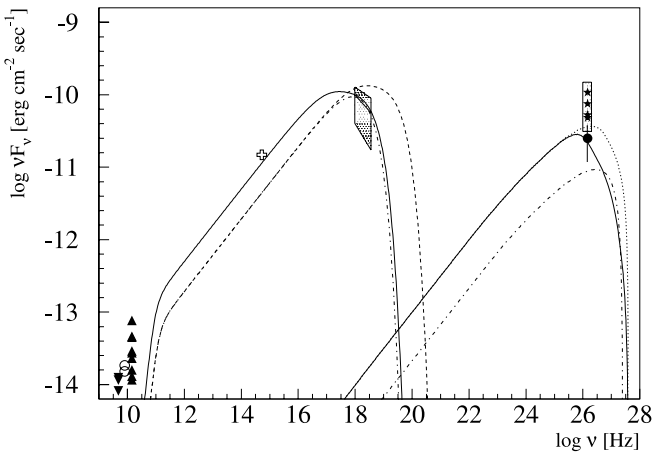

FIG. 5.—Radio to γ-ray SEDs of the blazar 1ES 1959+650. All the radio fluxes observed between 2003 May 2 and June 7 are shown (UMRAO). The downward-pointing triangles are 4.8 GHz, the open circles are 8.0 GHz, and the upward-pointing triangles are the 14.5 GHz radio data. The optical data point (*plus sign*) shows the flux detected on 2003 June 7 (Bordeaux Observatory). The shaded region in the X-ray energy range shows the range of fluxes and energy spectra observed during the campaign with the *RXTE* satellite. The straight line in the middle is the mean X-ray spectrum, measured simultaneously with the TeV γ-ray observation. At TeV energies the range of upper limits is shown as a shaded region (i.e., the top of the shaded region is the highest upper limit, and the bottom of the region is the lowest upper limit) for the majority of the 28 minute Whipple observations, and flux estimates (*filled stars*) for the only four 28 minute Whipple observations that were strong enough to produce data points (rather than upper limits). The filled circle shows the average flux measured during the 2003 campaign in nights with *RXTE* observations. Three curves are shown: (1) the dashed line shows a SSC fit to an intermediate-flux-level SED observed during 2002 (see Paper I), (2) the dot-dashed line shows a SSC fit to the average X-ray spectrum observed during 2003, obtained with the same parameter values as (1) but with a reduced break energy and high-energy cutoff of the electron spectrum, and (3) the solid line shows the fit to the 2003 SED with freely varying SSC parameter values. All model parameter values are given in Table 2. The dotted line shows (3) without the effect of intergalactic γ-ray absorption. These three sets of model parameter values produce similar SEDs.

TABLE 2
PARAMETER VALUES FOR THE SSC MODEL OF THE 2002 AND 2003 SEDs

Year	Fit	δ[a]	B (Gauss)	R (m)	w_p[b] (ergs cm $^{-3}$)	log ($E_{\rm min}$ eV^{-1})[c]	log ($E_{\rm max}$ eV^{-1})[d]	log (E_b eV^{-1})[e]
2002.....	1	20	0.04×10^{-4}	14×10^{13}	0.014	3.5	12.2	11.45
2003[f].....	2	20	0.04×10^{-4}	14×10^{13}	0.014	3.5	11.70	11.41
2003.....	3	20	0.02×10^{-4}	27.2×10^{13}	0.010	3.5	11.90	11.10

[a] Doppler factor of plasma.
[b] Electron energy density.
[c] Minimum energy of electrons.
[d] Maximum energy of electrons.
[e] Energy at which electron spectrum index changes from a 2 to 3.
[f] Best fit for 2003 data with only log ($E_{\rm max}$ eV^{-1}) and log (E_b eV^{-1}) varied from 2002.

a rather low predicted TeV γ-ray flux. However, both (2) and (3) are consistent with the data. We discuss the SSC model fits further in § 6.

6. SUMMARY AND DISCUSSION

In this paper, we have presented the results of a multiwavelength campaign on the blazar 1ES 1959+650 carried out in 2003 May and June, 1 year after the major flaring phase of 2002. Our campaign did not reveal a statistically significant TeV γ-ray flare, and the highest X-ray fluxes observed during the 2003 campaign were lower by a factor of 5 than the highest fluxes observed in 2002. Contrasting the behavior of the source at high energies (X-rays and γ-rays), the optical and radio flux levels did not change from 2002 to 2003. The lack of a correlation between the high-energy (X-ray and γ-ray) and low-energy (radio and optical) flux levels observed in the years 2002 and 2003 suggests that the high-energy radiation is produced close to the central engine and that the low-energy radiation is produced farther downstream of the jet. Indeed, radio emission produced closer to the source would be self-absorbed and hence not visible. It is also possible that optical emission may come from "old" components that do not shine in X-rays anymore, but could in fact be closer to the central engine. The examination of a possible correlation between the TeV γ-ray flux and X-ray flux will benefit greatly from more-sensitive Cerenkov telescopes such as VERITAS or MAGIC (MAGIC detected 1ES 1959+650 in 2004 September and October in a state of low activity, with a significance of 8.2 σ after $\sim$6.0 hr of observations; Albert et al. 2006).

An interesting result from our campaign is that the 10 keV fluxes and 4–15 keV photon indices appear correlated during individual observation periods, but that the apparent correlation evolves on a timescale on the order of a year. In an initial attempt to identify whether a single model parameter might be responsible for the secular evolution, we varied individual SSC model parameters and studied the effect on a correlation between X-ray flux and photon index. Comparing the correlations resulting from varying individual model parameters (Fig. 6) with the apparent observed correlations (Fig. 3), one may speculate that individual flares on a timescale of days are caused by a variation of the Doppler factor δ, the magnetic field B, and/or E_b and that the secular evolution of the source on a timescale of months is caused by a shift of the maximum energy $E_{\rm max}$ to which electrons are accelerated. In a similar study of the blazar Mrk 501 (an object in many aspects similar to 1ES 1959+650), Tavecchio et al. (2001) also identified $E_{\rm max}$ as a likely parameter to cause long-term variations of the fluxes and energy spectra. The results discussed here should be taken with caution, as we cannot exclude that several jet parameters change simultaneously from flare to flare and on longer timescales.

Recently, Uttley et al. (2005) interpreted the flaring activity of AGNs as a red-noise process with significant power at low frequencies and a lognormal amplitude distribution. In this context, hourly and daily variations are considered high-frequency noise, and yearly variations are considered low-frequency noise. As the discussion above shows, secular evolutions of the emission characteristics may be able to shed light on the physical origin of the "power at low frequencies." Long-term monitoring on timescales of years may thus be equally crucial for understanding the inner workings of AGN jets as intensive observations on timescales of several weeks.

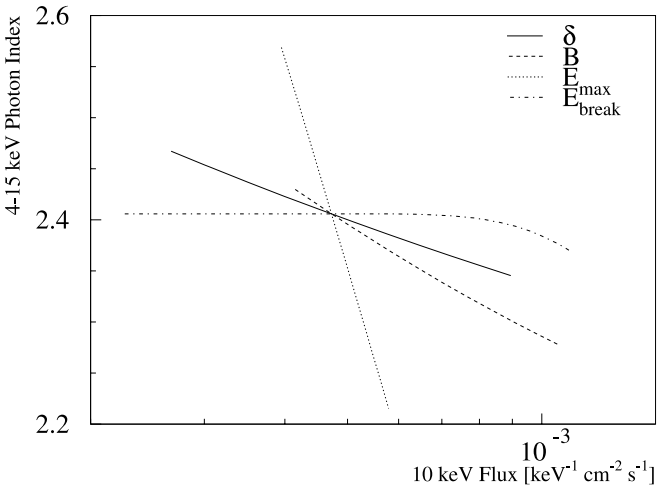

FIG. 6.—The 10 keV flux vs. 4–15 keV photon index correlation resulting from changing individual SSC model parameter values. All parameters not indicated are fixed to the values given in Table 2 (fit 3). *Solid line*: δ is varied from 17.63 to 23.09 left to right. *Dashed line*: The magnetic field B is varied from 0.019×10^{-4} to 0.028×10^{-4} G from left to right. *Dotted line*: The parameter log ($E_{\rm max}$ eV^{-1}) is varied from 11.84 to 12.02 top to bottom. *Dot-dashed line*: The parameter log (E_b eV^{-1}) is varied from 10.78 to 11.47 from left to right. The starting point for all model parameter values is given in Table 2, row 3.

This research is supported by the U.S. Department of Energy, the National Science Foundation, and the Smithsonian Institution; by NSERC in Canada; by Science Foundation Ireland; and by PPARC in the UK. K. G. and H. K. gratefully acknowledge support by NASA through grant NAG 13770 and support by the Department of Energy through the Outstanding Junior Investigator program. The University of Michigan Radio Astronomy Observatory (UMRAO) is partially supported by funds from the Michigan Department of Astronomy.

REFERENCES

Aharonian, F., et al. 1999, A&A, 342, 69
———. 2003, A&A, 406, L9
Albert, J., et al. 2006, ApJ, 639, 761
Becker, R. H., White, R. L., & Edwards, A. L. 1991, ApJS, 75, 1
Böttcher, M. 2005, ApJ, 621, 176
Charlot, P., & Le Campion, J.-F. 2004, in SF2A-2004: Semaine de l'Astrophysique Francaise, ed. F. Combes et al. (Les Ulis Cedex: EDP Sciences), 425
Daniel, M. K., et al. 2005, ApJ, 621, 181
Falcone, A. D., Cui, W., & Finley, J. P. 2004, ApJ, 601, 165
Giebels, B., et al. 2002, ApJ, 571, 763
Gregory, P. C., & Condon, J. J. 1991, ApJS, 75, 1011
Halzen, F., & Hooper, D. 2005, Astropart. Phys., 23, 537
Helene, O. 1983, Nucl. Instrum. Methods Phys. Res., 212, 319
Hillas, A. M., et al. 1998, ApJ, 503, 744
Holder, J., et al. 2003, ApJ, 583, L9
Kneiske, T. M., Mannheim, K., & Hartmann, D. H. 2002, A&A, 386, 1
Krawczynski, H. 2006, in ASP Conf. Proc. 350, Blazar Variability Workshop II: Entering the *GLAST* Era, ed. H. R. Miller et al. (San Francisco: ASP), in press (astro-ph/0508621)
Krawczynski, H., Coppi, P. S., Maccarone, T., & Aharonian, F. A. 2000, A&A, 353, 97
Krawczynski, H., et al. 2004, ApJ, 601, 151 (Paper I)
Pian, E., et al. 1998, ApJ, 492, L17
Schachter, J. F., et al. 1993, ApJ, 412, 541
Schroedter, M. 2005, ApJ, 628, 617
Tavecchio, F. 2006, in The Tenth Marcel Grossmann Meeting, ed. M. Novello, S. Perez-Bergliaffa, & R. Ruffini (Hackensack: World Scientific), in press (astro-ph/0401590)
Tavecchio, F., et al. 2001, ApJ, 554, 725
Uttley, P., McHardy, I. M., & Vaughan, S. 2005, MNRAS, 359, 345